International Journal of Radiology and Radiation Oncology

Wataru Kawakami[1,2]*, Akihiro Takemura[2], Kunihiko Yokoyama[3], Kenichi Nakajima[4], Tetsu Nakaichi[1], Shoichi Yokoyama[1] and Kichiro Koshida[2]

[1]Department of Radiological Technology, Public Central Hospital of Matto Ishikawa, Ishikawa, Japan
[2]Department of Quantum Medical Technology, Division of Health Sciences, Graduate School of Medical Science, Kanazawa University, Ishikawa, Japan
[3]PET Imaging Center, Public Central Hospital of Matto Ishikawa, Ishikawa, Japan
[4]Department of Nuclear Medicine, Kanazawa University Hospital, Ishikawa, Japan

Dates: Received: 18 September, 2015; **Accepted:** 19 October, 2015; **Published:** 21 October, 2015

***Corresponding author:** Wataru Kawakami, Department of Radiological Technology, Public Central Hospital of Matto Ishikawa, 3-8, Kuramitsu, Hakusan City, Ishikawa, Japan; Tel: +81-76-275-2222; Fax: +81-76-274-5974; E-mail: rt01@mattohp.com

www.peertechz.com

Keywords: Cone beam computed tomography; Limited angle of projections; Image registration; Conventional radiotherapy; Image-guided radiotherapy

Research Article

Application of Cone Beam Computed Tomography to Conventional Radiotherapy: Limited Angle of Projections for Lymph Nodes Located above or below the Collarbone

Abstract

Various techniques are used in image-guided radiotherapy (IGRT). Cone beam computed tomography (CBCT) is widely used in IGRT on linear accelerators. The increased accuracy of IGRT enables reducing planning target volume margins and doses to normal tissues. However, for radiation therapies requiring fractionated irradiation, increased exposure dose attributed to CBCT becomes problematic. We investigated the smallest projection angle required to provide target accuracy for CBCT of lymph nodes located above or below the collarbone in breast cancer patients.

Phantom and clinical experiments were conducted on the basis of shifts obtained through gray value-based auto-image registration performed using 360° CBCT. Corrected images obtained from decreasing projection angles in 10° increments were compared with a single 360° image.

In the phantom and clinical experiments, the smallest projection angle used as the tolerance level were 80° and 100°, which yielded the same accuracy as the 360° case. When irradiating lymph nodes above or below the collarbone with CBCT, a 100° projection angle was necessary for auto-image registration, whereas a projection angle of 195.8° (180° + fan) was required to produce artifact-free images.

This represents 95.8° reductions in the projection angle, resulting in a 48.9% reduction in exposure.

Abbreviations

IGRT: Image-Guided Radiotherapy; CBCT: Cone Beam Computed Tomography; RT: Radiotherapy; FOV: Field-Of-View

Introduction

Image-guided radiotherapy (IGRT) is indispensable for ensuring high accuracy of modalities such as intensity-modulated radiotherapy (RT) and stereotactic RT. Computed tomography, magnetic resonance imaging, ultrasound, and X-ray imaging techniques are used as part of the IGRT approach. In addition, cone beam computed tomography (CBCT) has been widely used in IGRT on linear accelerators [1]. CBCT is used to obtain images immediately before or during treatment, and it corrects any discrepancies between the treatment plan and the resulting image. The increased accuracy of IGRT allows for reductions in the planning target volume margin and doses to normal tissues [2]. However, in radiation therapies requiring fractionated irradiation, the increase in the exposure dose attributable to CBCT becomes a serious problem [3,4]. In addition, neither guidelines nor dose constraints for radiation exposure resulting from CBCT exist at present.

IGRT is effective not only in highly accurate treatment but also as a component of conventional RT. Conventional RT may be used to treat lymph nodes above or below the collarbone. For patients with breast cancer and ≥4 auxiliary lymph node metastases [5], additional RT to the lymph nodes above or below the collarbone is recommended as part of a conservative therapeutic strategy. For cases in which <4 auxiliary lymph node metastases are present, the need for additional RT to the lymph nodes above or below the collarbone is determined according to the patient's health details. However, vital organs such as the trachea, esophagus, and spinal cord are adjacent to these lymph nodes, and errors related to accurate delivery of radiation to the lymph nodes in this region can be caused by the positioning of the arm and jaw [6].

This study aimed to effectively utilize IGRT for conventional RT of the lymph nodes above or below the collarbone. To deliver highly accurate RT, corrections must be made according to the body position and orientation of internal organs. To obtain information related to organ orientation, an artifact-free image is required and procured using a minimum CBCT projection angle of 180° + fan [7,8]. However, accurate RT on the lymph nodes above or below

the collarbone requires the selected image to be corrected for the body position. Examination of the necessary projection angle is therefore crucial in reducing radiation exposure [9,10]. In this study, we investigated the limited angle of projections for the auto-image registration of lymph nodes located above or below the collarbone in patients with breast cancer.

Materials and Methods

Image acquisition

Image acquisition was performed using a linear accelerator equipped with a kV imaging device (Synergy, Elekta Inc., Crawley, UK). The commercial clinical algorithm XVI R4.5.1 (Elekta, Inc.) was used for image reconstruction and registration, and images were acquired at a 360° angle. The irradiation head, which was pointed vertically downward, displayed 0° and was rotated from −180° to 180° (clockwise) or from 180° to −180° (counter-clockwise). The gantry speed was 60 s per rotation, and the resolution of each projection image was 512 × 512 pixels. The XVI reconstruction algorithm used was Feldkamp's back-projection algorithm, which applies a flex-map correction to the rotation orbits [11]. For CBCT imaging, the kV panel can be positioned laterally (using motorized movements) at 3 different field-of-view (FOV) positions: S, M, and L (small, medium, and large, respectively). The panel was placed in the S FOV position for this study. The kV central axis corresponded to the panel center with S, and the projection angle required was 195.8° (180° + fan) to yield an artifact-free image (Figure 1). Typical scanning parameters for the head and neck were used to acquire images for this study, with a tube voltage, tube current, duration per pulse, projected image number, fan angle, and collimator type of 100 kV, 10 mA, 10 ms, 360, 15.8°, and S20, respectively.

Phantom study

A female phantom, constructed using an authentic human skeleton cast inside a soft tissue-simulation material (SB-4-A; Kyoto Kagaku, Fushimi-ku, Kyoto, Japan), was selected as a rigid imaging object for our registration accuracy study. A virtual plan was made from reference CT images acquired using multi-slice CT (Activion16; Toshiba, Tokyo, Japan). The Xio 4.80 (Elekta, Inc.) RT-planning device was used. After the phantom was positioned on the treatment table, the isocenters of the virtual plan and the phantom were corrected using CBCT. Subsequently, CBCT was performed after remote movements of 0, +1, or −1 cm from each axis [with axis parameters of Lat(X), Lng(Y), and Vrt (Z), respectively] at a 360° rotation (Figure 1). Measurements were acquired at 26 positions relative to the virtual plan isocenter.

Clinical study

This study was approved by the ethics committees of the Public Central Hospital of Matto Ishikawa, and all the patients provided written informed consent. Image sets acquired from 8 patients were used in our registration study. Reference CT images were acquired for planning purposes using multi-slice CT 1 week before treatment, for planning purposes, and CBCT images were acquired immediately before treatment for registration with the reference CT images, for localization purposes. The amount of radiation dose received for each irradiation was assumed to be 2.0 Gy, the irradiation frequency was 25 repeats, and CBCT was performed in 10 sets of 25 repeats. As many as 80 datasets obtained from 8 patients whose lymph nodes were irradiated above or below the collarbone were acquired as follows: right lymph nodes above or below the collarbone, taken from 5 patients, 10 repeats per patient; left lymph nodes above or below the collarbone, taken from 3 patients, 10 repeats per patient. All the patients were supine, with both arms raised using an arm support (MT-WB09; Civco, Iowa, USA). The right and left sides of the body were labeled clockwise and counter-clockwise, respectively, relative to the direction of rotation.

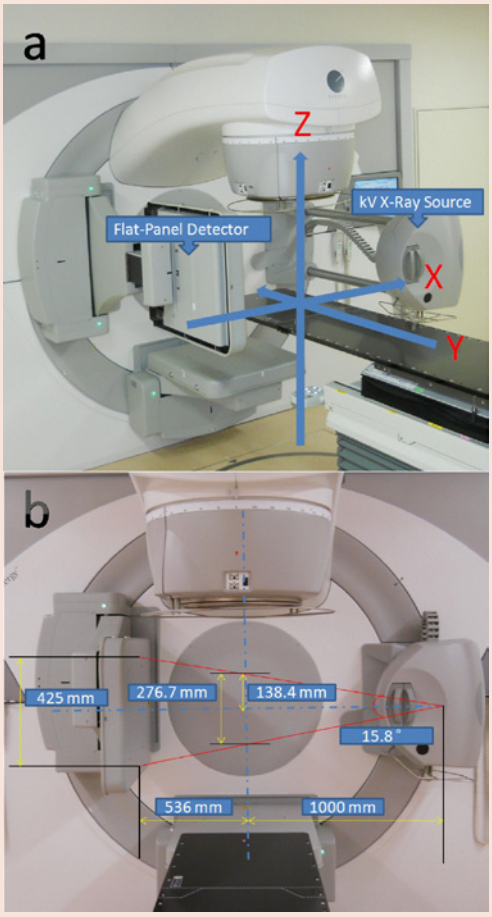

Figure 1: Images of a linear accelerator equipped with a kV imaging device. (a) X, Y, and Z are the lateral, anteroposterior, and vertical directions, respectively. (b) The fan angle is 15.8° at a distance from the kV X-ray source and flat-panel detector.

Data analysis

The data were analyzed according to the residual errors for gray value-based auto-image registration performed using 360° CBCT. The XVI algorithm provided manual and point-based image registration using bony-based and gray value-based automated image registration methods [12]. A comparison based on the residual error was then made using the corrected image (the projection angle decreased in 10° increments), following which the image was recomposed.

Citation: Kawakami W, Takemura A, Yokoyama K, Nakajima K, Nakaichi T, et al. (2015) Application of Cone Beam Computed Tomography to Conventional Radiotherapy: Limited Angle of Projections for Lymph Nodes Located above or below the Collarbone. Int J Radiol Radiat Oncol 1(1): 014-018. DOI: http://dx.doi.org/10.17352/ijrro.000005

The residual error was defined by its absolute value, regardless of orientation. Because image reconstruction was impossible for projection angles ≤30°, the projection angle was evaluated in the range of 40–360°. The adverse event to be mainly avoided during treatment is myelopathy, although the head and neck region contains other organs at risk. Therefore, the distance between the contour line of the 80% dose (40 Gy) and the beginning of the spinal cord was measured, yielding a shortest distance of 0.63 mm. The upper-bound value of the permitted error margin was set to half this value (0.3 mm) for the present study. The smallest projection angle for the average of residual errors, plus 2 standard deviations (2 SDs), was determined.

Results

In the phantom experiment, the average of residual errors, plus 2 SDs, varied by <0.3 cm along each axis at the following projection angles: X-axis, ≥80° (Figure 2); Y-axis, ≥80° (Figure 3); Z-axis, ≥60° (Figure 4). The smallest projection angle used as the tolerance level for the 3 axes was 80°, yielding the same accuracy as the 360° case. Patient analysis yielded values, plus 2 SDs, which varied by <0.3 cm at the following projection angles: X-axis, ≥90° (Figure 2); Y-axis, ≥90° (Figure 3); Z-axis, ≥100° (Figure 4). The smallest projection angle used in this case was 100°, yielding the same accuracy as the 360° case. The smallest angle of projections used in the phantom experiment employed an 80° gantry rotation, whereas a 100° gantry rotation was required for patient analyses. Because it was difficult to perform manual image registration using images acquired at 80° and 100°, automated registration was required (Figure 5). A projection angle of 195.8° (180° + fan) is normally required to produce artifact-free images. A limited projection angle of 100° represents a decrease of 95.8°, leading to a potential decrease of 48.9% in exposure.

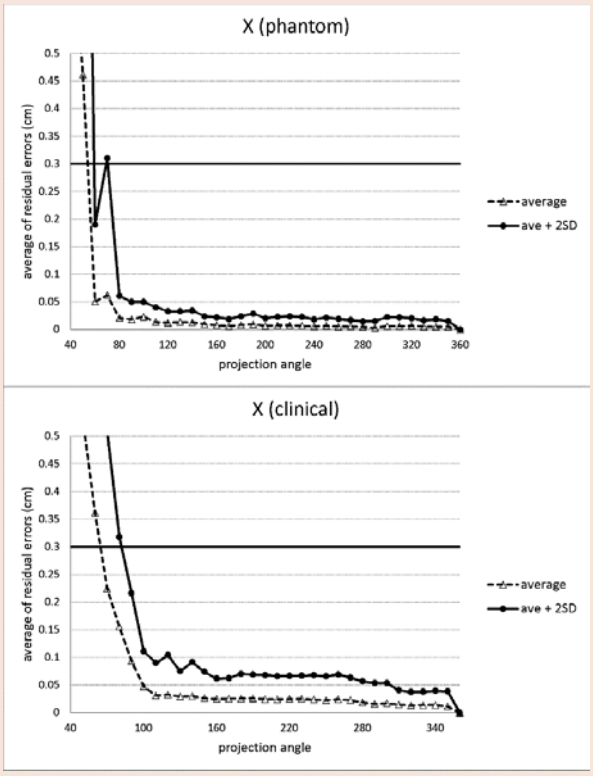

Figure 2: Average of residual errors in terms of the CBCT projection angle along the X-axis. The phantom experiment average of residual errors plus 2 standard deviations (ave + 2 SD) varied by <0.3 cm along the X-axis at projection angles of ≥80° gantry rotation. Patient analysis yielded ave + 2 SD values that varied by <0.3 cm at projection angles of ≥90° gantry rotation.

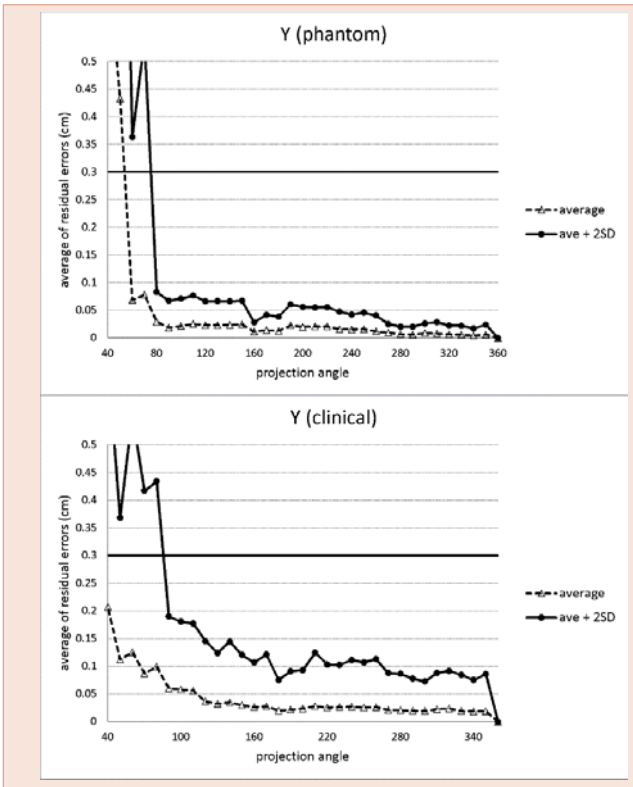

Figure 3: Average of residual errors in terms of the CBCT projection angle along the Y-axis. The phantom experiment average of residual errors plus 2 standard deviations (ave + 2 SD) varied by <0.3 cm along the Y-axis at projection angles of ≥80° gantry rotation. Patient analysis yielded ave + 2 SD values that varied by <0.3 cm at projection angles of ≥90° gantry rotation.

Discussion

The source of the large 2 SDs may be explained by comparing the Y- and Z-axes with the X-axis in both the phantom and clinical experiments. Resolution along the body axis tends to decrease because Feldkamp's method employs a wide detection side for the projection data in each slice. Therefore, the Y-axis (body axis) 2 SDs were greatly influenced by a data shortage resulting from a decrease in the projection angle. Moreover, a streak artifact that excluded the rotation center slice resulting from a data shortage along the orientation corresponding to the beginning and end of data collection, at projection angles of ≤200°. It is thought that this led to an increase in the 2 SDs of the Z-axis (Figure 5).

The 2 SDs of the clinical data were larger than those of the phantom data, possibly because of physical differences in the body at each point of clinical data acquisition. In addition, poor image quality

Citation: *Kawakami W, Takemura A, Yokoyama K, Nakajima K, Nakaichi T, et al. (2015) Application of Cone Beam Computed Tomography to Conventional Radiotherapy: Limited Angle of Projections for Lymph Nodes Located above or below the Collarbone. Int J Radiol Radiat Oncol 1(1): 014-018. DOI: http://dx.doi.org/10.17352/ijrro.000005*

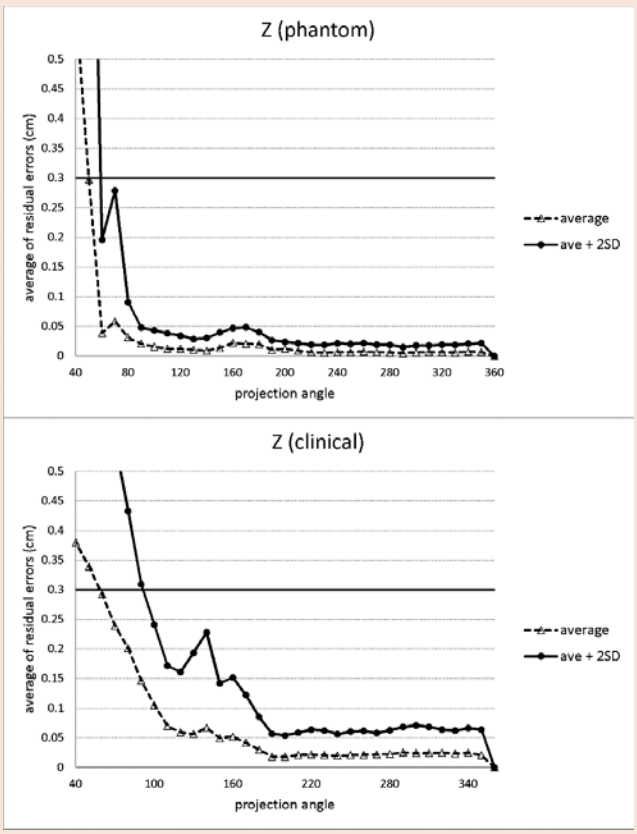

Figure 4: Average of residual errors in terms of the CBCT projection angle along the Z-axis. The phantom experiment average of residual errors plus 2 standard deviations (ave + 2 SD) varied by <0.3 cm along the Z-axis at projection angles of ≥60° gantry rotation. Patient analysis yielded ave + 2 SD values that varied by <0.3 cm at projection angles of ≥100° gantry rotation.

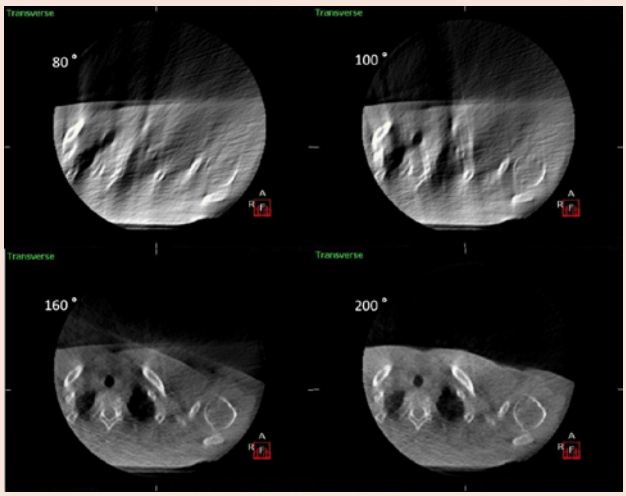

Figureu 5: Artifacts caused by differences in projection angle. (a) At 80°, artifacts may be observed on the body surface and the internal structure is not clear. (b) At 100°, artifacts are present on the body surface and the internal structure is not clear. (c) At 160°, the contour is expanded along the Z-axis and artifacts can be observed. However, the internal structure is clear. (d) At 200°, there are no artifacts on the body surface and the internal structure is clear.

caused by the increased sizes of the covered patients compared with the phantom may have been a contributing factor.

Here, the upper bound of the permitted error margin value was 0.3 cm. However, as the total treatment frequency, beam position, and organs at risk differ according to prevailing circumstances in other regions of the body, a limited projection angle of 100° is not the only available, or necessary, option.

Because residual set-up errors larger than 5 mm were observed on average in 18% to 27% of all fractions of patients treated in the chest, abdomen and pelvis, and in 10% of fractions of patients treated in the head and neck [13], it is necessary to correct the set-up error by CBCT in conventional RT. Therefore, it is important to investigate the limited angle of projections for the auto-image registration. The results of this study indicate that the projection angle may possibly be decreased for use in other regions of the body. Moreover, an investigation of the influences of tube voltages and currents on registration is required. It appears that exposure could be further decreased by adding various evaluations, although only the effect of the projection angle was investigated in the present study.

Conclusion

The use of CBCT to irradiate lymph nodes located above or below the collarbone required a limited projection angle of 100° for auto-image registration. This represents a reduction of 95.8° compared with the standard projection angle, resulting in a possible reduction in exposure of 48.9%. In the future, it will be possible to use CBCT for IGRT with conventional RT by determining the limited angle of projections required for the image registration of various regions of the body.

References

1. Jaffray DA, Siewerdsen JH, Wong JW, Martinez AA (2002) Flat-panel cone-beam computed tomography for image-guided radiation therapy. Int J Radiat Oncol Biol Phys 53: 1337–1349.

2. Yeung AR, Li JG, Shi W, Newlin HE, Chvetsov A, et al. (2009) Tumor localization using cone-beam CT reduces set up margins in conventionally fractionated radiotherapy for lung tumors. Int J Radiat Oncol Biol Phys 74: 1100–1107.

3. Song WY, Kamath S, Ozawa S, Ani SA, Chvetsov A, et al. (2008) A dose comparison study between XVI and OBI systems. Med Phys 35: 480–486.

4. Zhang Y, Yan Y, Nath R, Bao S, Deng J (2012) Personalized estimation of dose to red bone marrow and the associated leukaemia risk attributable to pelvic kilo-voltage cone beam computed tomography scans in image-guided radiotherapy. Phys Med Biol 57: 4599–4612.

5. Clarke M, Collins R, Darby S, Davies C, Elphinstone P, et al. (2005) Effects of radiotherapy and of differences in the extent of surgery for early breast cancer on local recurrence and 15-year survival: an overview of the randomised trials. Lancet 366: 2087–2106.

6. Lozano EM, Perez LA, Torres J, Carrascosa C, Sanz M, et al. (2011) Correction of systematic set-up error in breast and head and neck irradiation through a no-action level (NAL) protocol. Clin Transl Oncol 13: 34–42.

7. Gang GJ, Tward DJ, Lee J, Siewerdsen JH (2010) Anatomical background and generalized detectability in tomosynthesis and cone-beam CT. Med Phys 37: 1948–1965.

8. Kowatsch M, Winkler P, Zurl B, Konrad T, Schrottner J (2011) Analysis of image quality and dose calculation accuracy in cone beam CT acquisitions

Citation: *Kawakami W, Takemura A, Yokoyama K, Nakajima K, Nakaichi T, et al. (2015) Application of Cone Beam Computed Tomography to Conventional Radiotherapy: Limited Angle of Projections for Lymph Nodes Located above or below the Collarbone. Int J Radiol Radiat Oncol 1(1): 014-018. DOI: http://dx.doi.org/10.17352/ijrro.000005*

with limited projection data (half scan, half fan) with regard to usability for adaptive radiation therapy treatment planning. Z Med Phys 21: 11–18.

9. Lu B, Lu H, Palta J (2010) A comprehensive study on decreasing the kilovoltage cone-beam CT dose by reducing the projection number. J Appl Clin Med Phys 11: 3274.

10. Stieler F, Wenz F, Shi M, Lohr F (2013) A novel surface imaging system for patient positioning and surveillance during radiotherapy. A phantom study and clinical evaluation. Strahlenther Onkol 189: 938–944.

11. Feldkamp L, David L, Kreiss J (1984) Practical cone beam algorithm. J Opt Soc Am A 1: 612–619.

12. Maintz JB, Viergever MA (1998) A survey of medical image registration. Med Image Anal 2: 1–36.

13. Rudat V, Hammoud M, Pillay Y, Alaradi AA, Mohamed A, et al. (2011) Impact of the frequency of online verifications on the patient set-up accuracy and set-up margins. Radiat Oncol 6: 101.

Citation: *Kawakami W, Takemura A, Yokoyama K, Nakajima K, Nakaichi T, et al. (2015) Application of Cone Beam Computed Tomography to Conventional Radiotherapy: Limited Angle of Projections for Lymph Nodes Located above or below the Collarbone. Int J Radiol Radiat Oncol 1(1): 014-018. DOI: http://dx.doi.org/10.17352/ijrro.000005*